The effect of Ca substitution on the structure and the Raman active phonons in $Y_{1-x}Ca_xBa_2Cu_3O_{7-\delta}$

1998 J. Phys.: Condens. Matter 10 2515

(http://iopscience.iop.org/0953-8984/10/11/015)

J. Phys.: Condens. Matter **10** (1998) 2515–2524. Printed in the UK PII: S0953-8984(98)89635-5

The effect of Ca substitution on the structure and the Raman active phonons in $Y_{1-x}Ca_xBa_2Cu_3O_{7-\delta}$

D Palles†, E Liarokapis†, Th Leventouri‡ and B C Chakoumakos§

† Department of Physics, National Technical University, Athens 157 80, Greece
‡ Department of Physics, Florida Atlantic University, Boca Raton, FL 33431, USA
§ Solid State Division, Oak Ridge National Laboratory, Oak Ridge, TN 37831-6393, USA

Received 27 November 1997

Abstract. Micro-Raman measurements and Rietveld refinements of x-ray data have been carried out in the superconducting system $Y_{1-x}Ca_xBa_2Cu_3O_{7-\delta}$ with $0 \leqslant x \leqslant 0.12$, to delineate the effect of the excess doping on the Raman active phonons and especially on the characteristics of the plane oxygen modes. The increase of the Cu(2)–O(4) bond length with increasing Ca concentration induces a much smaller decrease in the frequency of the A_g phonon of the apical O(4) atom than the rare earth substitutions for Y. The frequency of the in-phase A_g vibrations of the plane oxygens decreases slightly with increasing Ca content, but remains well above the lowest value that has been reported for the oxygen overdoped pure $YBa_2Cu_3O_{7-\delta}$ compound, suggesting that the softening of this mode observed in those samples may not be attributed to the addition of carriers. The frequency of the out-of-phase B_{1g}-like vibrations of the plane oxygens is not affected by the substitution, but the width of the corresponding phonon increases considerably. This increase is due to the appearance of another mode of B_{1g} symmetry that could correspond to a hypothetical $CaBa_2Cu_3O_{7-\delta}$ phase separated from the pure YBCO phase.

1. Introduction

Ca^{2+} substitution at the Y^{3+} site of the $Y_{1-x}Ca_xBa_2Cu_3O_{7-\delta}$ system lowers the superconducting transition temperature in optimally oxygenated samples [1], and increases it in the oxygen-deficient ones [2] due to the excess of doping introduced by the substitution.

Raman measurements have shown a characteristic softening of the phonon mode due to the in-phase vibrations of the O(2,3) oxygens in the CuO_2 planes [3] in pure $YBa_2Cu_3O_y$ doped beyond the optimum value ($y \approx 6.92$) [4]. The same amount of softening in the overdoped region has been observed in samples where ^{18}O has been substituted for ^{16}O [5]. To further investigate any connection of this softening with the carrier doping we use an alternative way of changing the number of carriers by substituting Ca^{2+} in the Y^{3+} sites in the $Y_{1-x}Ca_xBa_2Cu_3O_{7-\delta}$ compound. Although the substitution of Ca for Y has been studied by many researchers [1, 2, 6, 7] and for various oxygen concentrations, no complete Raman data for all five strong ($4A_g + 1B_{1g}$) phonons of the material were up to now available to allow a comprehensive study of the consequence of doping on the phonon characteristics. The effect of such substitutions on the structure of samples in the $Y_{1-x}Ca_xBa_2Cu_3O_{7-\delta}$ system with $0 \leqslant x \leqslant 0.12$, is also investigated from the Rietveld refinement of the x-ray data. The modifications introduced in the interatomic distances is compared with the changes of the phonon characteristics and the earlier observed modifications in the Raman spectra by oxygen doping of $YBa_2Cu_3O_{7-\delta}$ [3, 5] and the rare earth substitutions for yttrium [8].

0953-8984/98/112515+10$19.50

2. Experiment

2.1. Sample preparation and characterization

The samples were synthesized with nominal Ca concentrations $x = 0.00$, 0.02, 0.05, 0.08 and 0.12, by the ordinary solid state reaction method. Appropriate amounts of high-purity Y_2O_3, $BaCO_3$, CuO, and $CaCO_3$ powders were mixed, calcined at 900 °C in air for 12 hours, and pressed into pellets. The pellets were heat-treated three times at 950 °C in air for 12 hours with intermediate grindings and pressings. Finally, they were heat-treated at 480 °C for 16 hours in flowing oxygen. Special care was taken during the preparation of the samples to keep identical preparation parameters, so that the oxygen concentration could be considered to be roughly the same in all samples. Indeed, the value of oxygen content, $7 - \delta$, as determined by iodometric titration measurements, was found to be approximately 6.9.

The critical transition temperatures were determined from a.c. magnetic susceptibility measurements with an estimated error ±1 K, and are listed in table 1. Figure 1 shows that $T_{c,\ onset}$ decreases monotonically with the calcium concentration from 92 K to 80 K, as it is expected for fully oxygenated samples [1].

Table 1. Structural parameters for $Y_{1-x}Ca_xBa_2Cu_3O_{7-\delta}$ as obtained by x-ray diffraction at room temperature (RT). Numbers in parentheses denote the standard deviation.

Nominal Ca (x)	0	0.02	0.05	0.08	0.12
Refined Ca (x)			0.029(13)	0.091(13)	0.104(15)
T_c (K)	92	90	86	83	81
a (Å)	3.8180(1)	3.8196(1)	3.8207(1)	3.8228(1)	3.8221(1)
b (Å)	3.8844(1)	3.8851(1)	3.8840(1)	3.8835(1)	3.8793(1)
c (Å)	11.6817(3)	11.6862(3)	11.6889(2)	11.6915(2)	11.6843(3)
z Ba	0.183 63(14)	0.183 68(14)	0.184 71(14)	0.184 69(15)	0.184 80(17)
z Cu(2)	0.353 86(30)	0.357 88(33)	0.355 57(27)	0.354 96(28)	0.355 17(31)
Cu(2)–O(2) (Å)	1.941(3)	1.920(1)	1.935(2)	1.930(2)	1.931(2)
Cu(2)–O(3) (Å)	1.958(2)	1.950(1)	1.957(2)	1.967(2)	1.950(2)
Cu(2)–O(4) (Å)	2.269(20)	2.298(20)	2.340(20)	2.321(20)	2.390(20)
R_w	0.0995	0.0804	0.0799	0.0846	0.0764
R_p	0.078	0.029	0.0616	0.0657	0.0586
x^2	2.027	1.826	1.801	2.022	1.390
CuO_2 buckling angle (°)	159.3(8)	168.4(8)	161.9(7)	164.2(8)	163.5(9)
Cu(1)–O(1) (Å)	1.942 22(6)	1.942 57(5)	1.942 02(4)	1.941 76(4)	1.939 66(5)
Cu(1)–O(4) (Å)	1.865(16)	1.884(17)	1.816(16)	1.829(16)	1.760(17)
Ba–Y (Å)	3.6958(16)	3.6966(17)	3.6854(16)	3.6864(17)	3.6829(20)

2.2. Structural studies

X-ray powder diffraction data were collected with a D5000 Siemens diffractometer with graphite monochromator and Cu Kα radiation. No secondary phases were detected. The diffraction patterns were refined with the General Structure Analysis Systems (GSAS) [9] program. The refinements were performed in the space group *Pmmm* [10] with isotropic temperature factors. The occupancy factor of the Y site was refined for the various concentrations and the refined Ca contents are used in the figures. The standard deviations (±0.013) of the refined Ca concentrations, shown in figures 1, 3 and 4, suggest that the actual substitution of calcium for yttrium is smaller than the nominal for the samples with 5

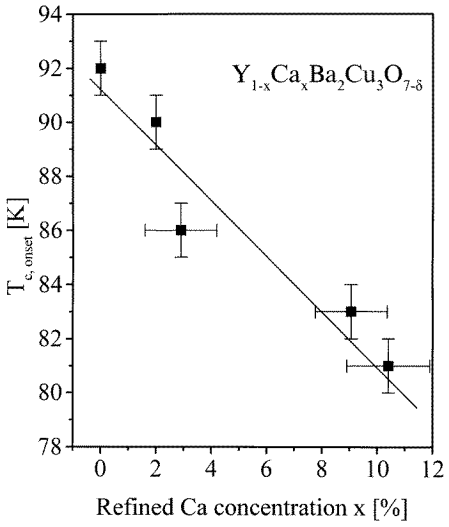

Figure 1. The dependence of the critical transition temperature $T_{c,\,onset}$ on the Ca concentration.

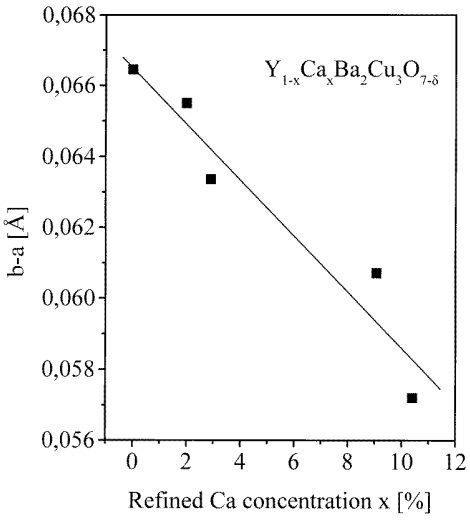

Figure 2. The orthorhombicity $(b-a)$ decreases as Ca enters in the Y sites. Standard deviations on the y axis do not show in this scale.

and 12% nominal concentration in calcium. The diffraction patterns from the samples with the various calcium concentrations were finally refined simultaneously for 24 variables, and results for lattice parameters, refined atomic positions z (as allowed by symmetry), bond lengths and weighted residuals R_w are listed in table 1. The lattice parameters of the samples do not show large variations with the Ca concentration, in agreement with previous publications [6, 7]. A small increase in the a axis, and a small decrease in the b axis is noticed. The c axis increases by a small amount also, which indicates that Ca^{2+} enters the Y^{3+} (1.02 Å) sites with an eightfold coordination (1.12 Å), instead of sixfold (1.0 Å) that the ionic sizes of these two atoms could suggest. The small but systematic decrease of the orthorhombicity $(b-a)$ with increasing doping is shown in figure 2.

The interatomic distances in the conductivity plane are shown in figure 3. The Cu(2)–O(2) and Cu(2)–O(3) bond lengths remain practically constant, whereas the Cu(2)–O(4) distance monotonically increases as more Ca^{2+} replaces the Y^{3+}. Figure 4 shows the monotonically decreasing Cu(1)–O(4) bond length with increasing Ca concentration, while the distance between the Cu(1) of the chains and Cu(2) of the planes remains approximately constant, indicating that O(4) (which bridges the chains with the planes) moves away from the conductivity plane and charge leaves the conducting planes as calcium increasingly occupies the yttrium sites. Figure 4 also illustrates that the interatomic distances Cu(1)–O(1) in the chains remain unaffected by the substitution, supporting the result of the iodometric titration measurements for approximately the same oxygen concentration in all samples.

The possibility of Ca substitution for Ba should have comparable effects with those of Sr substitution for Ba. The Sr ion size has an intermediate value between those of Ba and Ca, and in the case of the replacement of Ba by Sr, the O(4) atoms are brought closer to the CuO_2 planes [11], while here the opposite effect is observed (table 1). This suggests that Ca does not substitute for Ba, a conclusion also supported by the Raman results presented below.

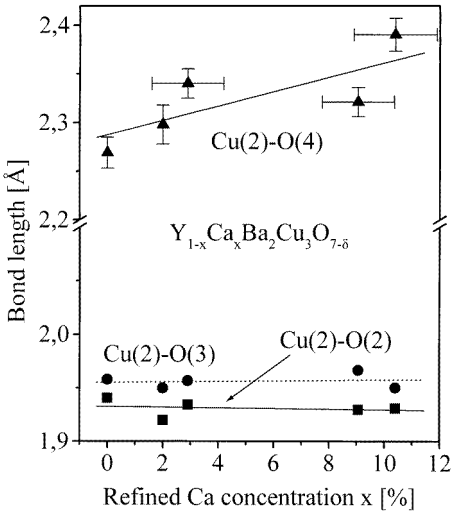

Figure 3. Interatomic distances between Cu(2) and the oxygen atoms versus the Ca concentration. Filled circles represent the Cu(2)–O(3) bond lengths, squares the Cu(2)–O(2) and the triangles correspond to the Cu(2)–O(4) distances.

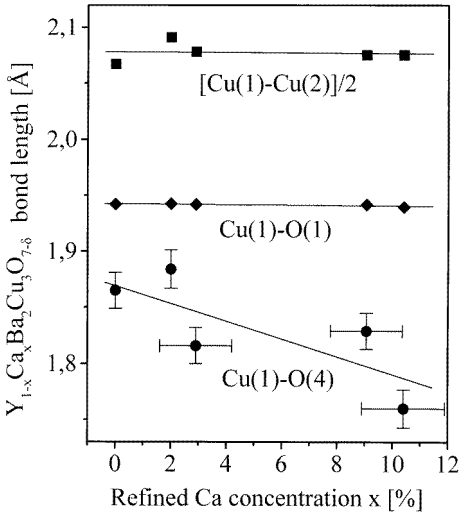

Figure 4. The Cu(1)–O(4) bond length (filled circles) decreases with the Ca concentration, while the bond lengths Cu(1)–O(1) (diamonds), as well as the distances between the Cu(2) of the planes and the Cu(1) of the chains (squares), remain unchanged.

2.3. Raman measurements

The Raman spectra of the samples were measured with a Jobin–Yvon triple spectrometer equipped with a liquid-N_2 cooled CCD and a microscope. The $y(xx)\bar{y}$ and $y(zz)\bar{y}$ scattering configurations, with the y and x axes located in the ab plane and z in the c axis, were obtained by adopting the classical backscattering geometry and by employing a polarizer and an analyser. The 488.0 and 514.5 nm lines of an Ar^+ laser were used for excitation at a power of <0.2 mW through a $\times 100$ objective lens producing a laser spot of approximately $1\,\mu$m diameter. At least three microcrystallites from each sample were measured and the spectra are shown in figures 5 and 6 for the $y(zz)\bar{y}$ and $y(xx)\bar{y}$ scattering configurations respectively. The frequencies and the widths of the strong Raman active modes of A_g or B_{1g} symmetry versus the refined calcium concentration are shown in figures 7 and 8.

Figure 7 shows that the frequency of the Ba mode is not affected by the Ca substitution while the frequency of the Cu(2) atom slightly decreases. In the case of Ba substitution by Sr, the Ba mode was found to shift continuously with increasing Sr concentration [11]. As Ca is an atom lighter than Sr, any substitution for Ba would induce stronger shifts in its phonon frequency (~ 2 cm^{-1} for the $x = 0.10$ sample). The absence of any shift or any other mode at a frequency corresponding to the mass difference of the two atoms is an indication that Ca does not substitute in considerable amounts for Ba.

The width of the Ba atom presented in figure 8 has been calculated from the Fano shape fitting of the data in the scattering configuration $y(xx)\bar{y}$, because an additional mode appears in the $y(zz)\bar{y}$ geometry around 126 cm^{-1}, as can be seen in figure 5. This additional mode has been also reported [5] for oxygen deficient pure $YBa_2Cu_3O_x$, and appears to be a disorder induced mode which is strong only in the $y(zz)\bar{y}$ geometry. There is a slight increase of the phonon widths for both Ba and Cu(2) atoms, but they are of small size and the study of the oxygen deficient pure $YBa_2Cu_3O_x$ has shown [5] it could be due to small

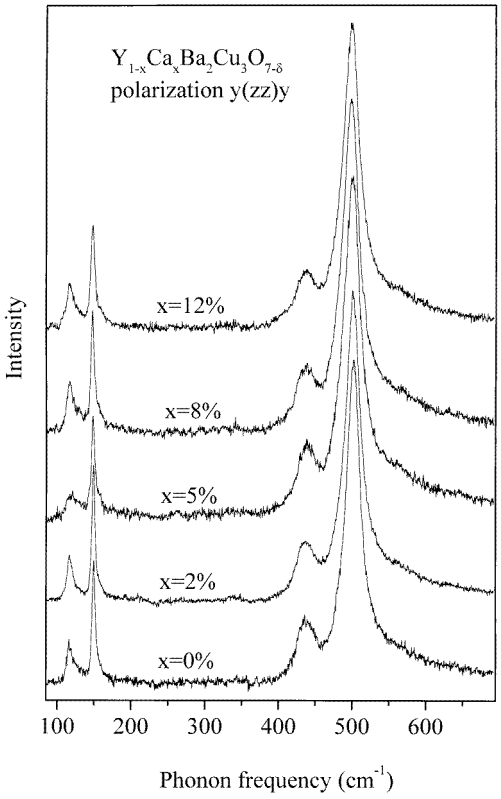

Figure 5. Characteristic Raman spectra in the $y(zz)\bar{y}$ scattering configuration.

differences in the amount of oxygenation between the samples. The relative intensities of the Ba and Cu(2) modes and the Fano asymmetry [12] of the Ba mode in the $y(xx)\bar{y}$ scattering configuration also vary among the different concentrations, possibly reflecting the slight differences in their oxygen content [3]. Similar conclusions can be drawn from the behaviour of the phonon characteristics of the Cu(2) atom (figures 7 and 8) [5].

Concerning the oxygen modes (figure 7), the frequency of the out-of-phase vibrations of the O(2,3) oxygens (B_{1g} mode) remains constant (or increases very slightly), which correlates with the stability of the Cu(2)–O(2,3) bond lengths upon Ca substitution (figure 3). On the other hand, the variation of the width of the B_{1g} mode is very large (18 to 25 cm^{-1}, figure 8). A careful examination of all spectra in the $y(xx)\bar{y}$ polarization reveals the presence of another mode at a lower frequency. The fitting of all spectra with two Fano lineshapes [12] of constant width and asymmetry induces the second mode at an approximately constant frequency of 323 cm^{-1} and of increasing relative intensity as shown in figure 9. Although the error bars are considerable in this figure, the linear fit to the results agrees remarkably well with the refined volumetric concentration of Ca (figure 9, dashed line). This second mode has the typical characteristics of a B_{1g} phonon due to the $CaBa_2Cu_3O_{7-\delta}$ compound, as it does not appear in the $y(zz)\bar{y}$ polarization, corresponds to the frequency of the hypothetical pure (and probably non-superconducting) $CaBa_2Cu_3O_{7-\delta}$ (as calculated using the corresponding Ca ionic radius from the trend of the $RBa_2Cu_3O_{7-\delta}$ compounds [13], where R is a rare earth), its relative intensity to the B_{1g} mode of Y-123 (induced from the

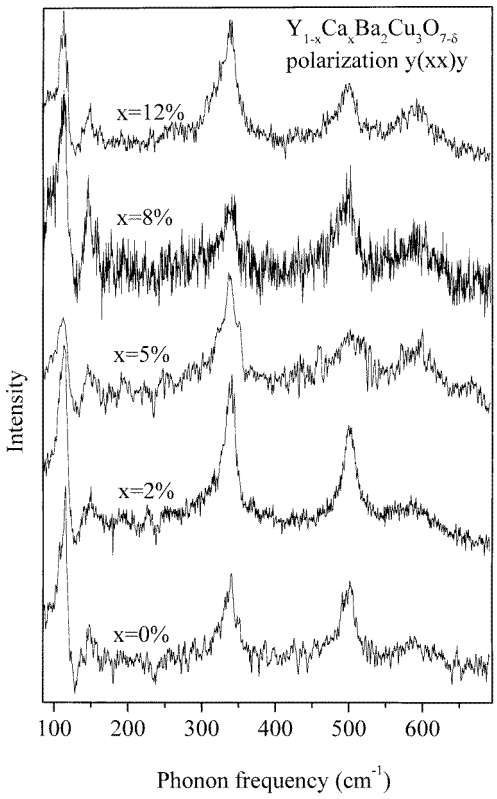

Figure 6. Characteristic Raman spectra in the $y(xx)\bar{y}$ scattering configuration.

double fitting) scales linearly with the amount of the Ca content (figure 9) and it does not appear in the oxygen deficient $YBa_2Cu_3O_{7-\delta}$ data [5] excluding any possibility of being due to an oxygen deficiency induced structural disorder. As reported [8], in the mixed rare earth compounds $Pr_{0.5}R_{0.5}Ba_2Cu_3O_{7-\delta}$, the B_{1g} oxygen phonon can be modified appearing as two or three modes related to the pure $PrBa_2Cu_3O_{7-\delta}$ or $RBa_2Cu_3O_{7-\delta}$ and a mixed phase, when there is a considerable difference in the ionic radii between Pr and the other rare earth. In the case of Ca substitution for Y, the same two-mode behaviour is expected as the ionic radius of Ca differs considerably from that of Y and the separation of the phase of pure Ca-123 seems a reasonable assumption supported by the data, though this pure phase cannot be prepared in stable form under normal conditions. Another possibility is to associate this mode with the one observed in ceramic $YBa_2Cu_3O_{7-\delta}$ samples under hydrostatic pressures [14]. In the present case of $Y_{1-x}Ca_xBa_2Cu_3O_{7-\delta}$ the larger size of Ca, as compared to that of Y, will induce an equivalent chemical pressure. If this new mode is also induced by the internal pressure, it should be present in the mixed rare earth substitution of Y which has not been observed [8].

In figure 7 it can be seen that the frequency of the in-phase vibrations of the plane oxygens of A_g symmetry decreases slightly with increasing amount of Ca, but always remains above 435 cm^{-1} which agrees with the practically unmodified bonds in the conducting planes. Comparison of these frequencies with the ones measured in the oxygen overdoped $YBa_2Cu_3O_x$ [3] indicates that the abrupt softening of this mode observed in [3]

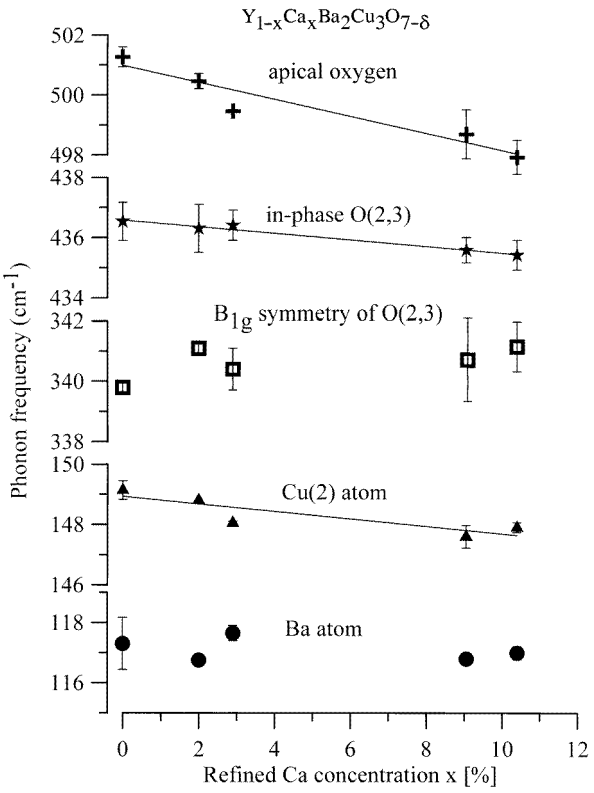

Figure 7. The dependence of the phonon frequencies on Ca concentration.

and [5] should not simply be due to the increase of the amount of carriers beyond optimum value, as it is not observed in the Ca overdoped samples. It should be rather related to structural modifications of the oxygen overdoped samples of a kind that does not appear in the Ca substituted samples, or with the possible existence of a secondary phase not related to the amount of doping. Concerning the width of the in-phase mode of the conductivity plane oxygens, it appears to be almost independent of the yttrium substitution (figure 8). In the pure Y-123 compounds the width of this mode was found to increase almost linearly with the amount of oxygen content. The value of the observed width is in agreement with other measurements which indicate near-optimally doped samples and with the other conclusions based on the Raman results as are the relative intensities of the Ba and Cu(2) modes in the $y(xx)\bar{y}$ scattering geometry discussed above.

Of all the modes, the frequency of the apical mode appears to be the most sensitive to the Ca substitution, decreasing with increasing calcium concentration. This behaviour can be related to the observed modifications in the structure, i.e. the decrease of the interatomic distance Cu(1)–O(4) and the increase of the Cu(2)–O(4) bond as shown in figures 3 and 4. It also matches closely the shift in the phonon frequency observed in the rare earth substitution of Y which is related to the size of the rare earth ion [13]. Taking into consideration the modification trend of the frequency of the apex phonon as measured in the $RBa_2Cu_3O_x$ compounds [13] and the size of the Ca ion, one can calculate a smaller shift ($\sim$1 cm^{-1}) for the maximum Ca substitution than the detected one ($\sim$4 cm^{-1}). This difference which is beyond any experimental error should be attributed to other than the size effects of the

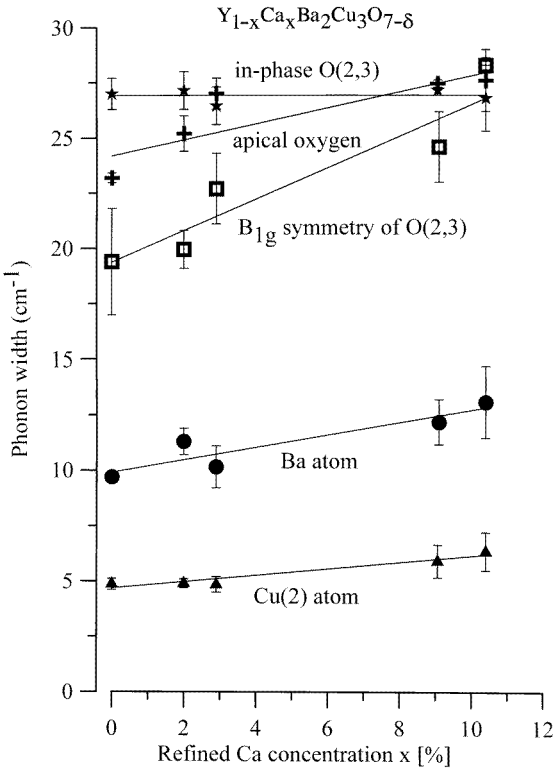

Figure 8. The dependence of the phonon widths on Ca concentration. For the B_{1g} phonon, a single Fano shape mode was assumed in this fit.

Ca substitution. Such effects could be related to the amount of overdoping induced by the substitution of the trivalent Y by the divalent Ca and the redistribution of carriers from the planes to the chains. The fact that the measured apex phonon frequency shift is not due to interatomic modifications only is also supported by its different dependence on the Cu(2)–O(4) or the Cu(1)–O(4) distances for the $Y_{1-x}Ca_xBa_2Cu_3O_{7-\delta}$ and $RBa_2Cu_3O_{7-\delta}$ compounds [13, 15]. Concerning the phonon width of the apical oxygen mode, it can be seen (figure 8) that it increases with the calcium concentration. This increase of the width is of the same amount ($\sim$4 cm^{-1}) and probably related to the shift of the frequency of the apex mode described before.

3. Conclusions

The substitution of Ca for Y in the $Y_{1-x}Ca_xBa_2Cu_3O_{7-\delta}$ system induces several modifications in the characteristics of the phonon modes as well as in the structural parameters.

Small variations of the frequency of the in-phase vibrations of the O(2,3) atoms of A_g symmetry are supported by practically constant bond lengths in the conducting planes, while the frequency remains above 435 cm^{-1} indicating that the previously reported softening of this mode, observed in the oxygen overdoped pure $YBa_2Cu_3O_{7-\delta}$ compound, may not be attributed to an increase of the carrier concentration, but should probably be associated with

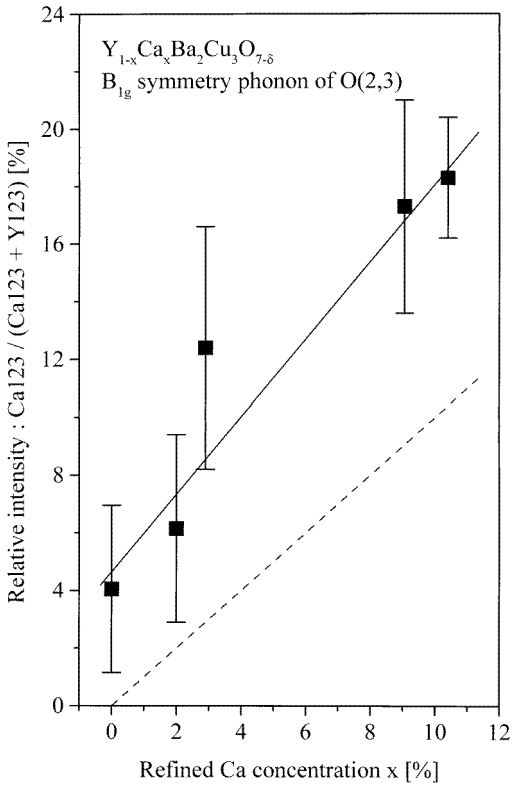

Figure 9. The relative intensity of the two B_{1g} modes as obtained by a fit with two Fano shape modes of constant widths and asymmetries corresponding to the hypothetical Ca123 and Y123. The dashed line ($y = x$) corresponds to the refined Ca concentration.

other effects.

The modifications in the width of the B_{1g} symmetry phonon are induced by the appearance of another mode in this scattering symmetry, which is correlated with the amount of Ca and possibly reflects the separation of the $CaBa_2Cu_3O_{7-\delta}$ phase that cannot be obtained in isolated form.

The significant decrease of the Cu(1)–O(4) bond length, the decrease of T_c and the increase of the Cu(2)–O(2)–Cu(2) bond angle indicate that carriers leave the conducting planes when Ca enters the Y sites. The frequency of the apical oxygen also decreases, but by a much smaller amount than expected from the substitution of a rare earth of similar size as Ca for Y, indicating the important role that the distribution of charges plays for the apex phonon.

Acknowledgments

This work was supported in part by a grant from ORISE, No S-3529. Oak Ridge National Laboratory is managed by Lockheed Martin Energy Research for the US Department of Energy under contract number DE-AC05-96OR22464. DP wishes to express his appreciation for financial support to the State Scholarships Foundation ('IKY') of Greece.

References

[1] Gledel C L, Marucco J F, Vincent E, Favrot D, Poumellec B, Touzelin B, Gupta M and Alloul H 1991 *Physica* C **175** 279
Awana V P S, Malik S K and Yelon W B 1996 *Physica* C **262** 272
[2] Manthiram A, Lee S J and Goodenough J B 1989 *J. Solid State Chem.* **73** 278
[3] Poulakis N, Palles D, Liarokapis E, Conder K, Kaldis E and Müller K A 1996 *Phys. Rev.* B **53** 534R
[4] Conder K, Zech D, Krüger C, Kaldis E, Keller H, Hewat A W and Jilek E 1994 *Phase Separation in Cuprate Superconductors* ed E Sigmund and K A Müller (Berlin: Springer)
[5] Palles D, Poulakis N, Liarokapis E, Conder K, Kaldis E and Müller K A 1996 *Phys. Rev.* B **54** 6721
[6] Awana V P S and Narlikar A V 1994 *Phys. Rev.* B **49** 6353
Awana V P S, Malik S K and Yelon W B 1996 *Physica* C **262** 272
[7] Böttger G, Mangelschots I, Kaldis E, Fischer P, Krüger C and Fauth F 1996 *J. Phys.: Condens. Matter* **8** 8889
[8] Bogachev G, Abrachev A, Iliev M, Poulakis N, Liarokapis E, Mitros C, Koufoudakis A and Psycharis V 1994 *Phys. Rev.* B **49** 12 151
[9] Larson A C and Von Dreele R B 1989 *GSAS—General Structures Analysis System* (Los Alamos National Laboratory)
[10] Williams A, Kwei G H, Von Dreele R B, Larson A C, Raistrick I D and Bish D L 1988 *Phys. Rev.* B **37** 7960
[11] Psycharis V, Mitros C, Koufoudakis A, Gamari-Seale H, Niarchos D, Kalitsounakis N, Poulakis N, Palles D and Liarokapis E 1996 *Physica* C **267** 211
[12] Fano U 1961 *Phys. Rev.* **124** 1866
[13] Rosen H J, Macfarlane R M, Engler E M, Lee V Y and Jacowitz R D 1988 *Phys. Rev.* B **38** 2460
[14] Syassen K, Hanfland M, Strössner K, Holtz M, Kress W, Cardona M, Schröder U, Prade J, Kulkarni A D and de Wette F W 1988 *Physica* C **153–155** 264
[15] Guillaume M, Allenspach P, Mesot J, Roessli B, Staub U, Fischer P and Furrer A 1993 *Z. Phys.* B **90** 13